López-Carrasco, MA.; Flores Pedauye, R. (2017). Dissecting the secondary structure of the circular RNA of a nuclear viroid in vivo: A "naked" rod-like conformation similar but not identical to that observed in vitro. RNA Biology. 14(8):1046-1054. doi:10.1080/15476286.2016.1223005

The predominant circular form of avocado sunblotch viroid accumulates *in planta* as a free RNA adopting a rod-shaped secondary structure unprotected by tightly bound host proteins

Amparo López-Carrasco and Ricardo Flores*

Instituto de Biología Molecular y Celular de Plantas (IBMCP), Universidad Politécnica de Valencia-Consejo Superior de Investigaciones Científicas, Valencia, Spain

Running title: *In vivo* SHAPE of a chloroplastic viroid RNA

Keywords: Circular RNAs, Non-coding RNAs, RNA secondary structure, SHAPE in vivo, Viroids

Abbreviations: *mc* and *ml,* monomeric circular and linear ASBVd RNA, respectively; PAGE, polyacrylamide gel electrophoresis; ASBVd, avocado sunblotch viroid; SHAPE, selective 2'-hydroxyl acylation analyzed by primer extension

*For correspondence (e-mail: rflores@ibmcp.upv.es)

The authors declare neither potential conflict of interest nor financial disclosure

ABSTRACT

Avocado sunblotch viroid (ASBVd), the type member of the family *Avsunviroidae*, replicates and accumulates in chloroplasts. Whether this minimal non-protein-coding, circular RNA of just 246-250 nt exists *in vivo* a free nucleic acid or closely associated with host proteins remains unknown. To tackle this issue, the secondary structures of the monomeric circular *(mc)* (+) and (-) strands of ASBVd have been examined *in silico* by searching those of minimal free energy, and *in vitro* at single-nucleotide resolution by selective 2'-hydroxyl acylation analyzed by primer extension (SHAPE). Both approaches resulted in predominant rod-like secondary structures without tertiary interactions, with the *mc* (+) RNA being more compact than its (-) counterpart as revealed by non-denaturing polyacryamide gel electrophoresis. Moreover, *in vivo* SHAPE showed that the *mc* ASBVd (+) form accumulates in avocado leaves as a free RNA adopting a similar rod-shaped conformation unprotected by tightly bound host proteins. Hence, the *mc* ASBVd (+) RNA behaves *in planta* like the previously studied *mc* (+) RNA of potato spindle tuber viroid, the type member of nuclear viroids (family *Pospiviroidae),* indicating that two different viroids replicating and accumulating in distinct subcellular compartments, have converged into a common structural solution. Circularity and compact secondary structures confer to these RNAs, and probably to all viroids, the intrinsic stability needed to survive in their natural habitats. However, *in vivo* SHAPE has not revealed the (possibly transient or loose) interactions of the *mc* ASBVd (+) RNA with two host proteins observed previously by UV irradiation of infected avocado leaves.

INTRODUCTION

Within viroids, small non-protein-coding circular RNAs capable of infecting and frequently inciting disease in certain higher plants (Diener, 2003; Flores et al., 2012; Palukaitis, 2014; Flores et al., 2015; Katsarou et al., 2015; Kovalskaya and Hammond, 2014; Steger and Perreault, 2016), avocado sunblotch viroid (ASBVd) (Palukaitis et al., 1979) displays two singular features: the smallest genomic size (246-250 nt) and an A+U content (62%) well above that of any other viroid (40-47%) (Symons, 1981; Flores et al., 2005; Owens et al., 2012). ASBVd, the type member of the family *Avsunviroidae,* replicates in plastids (mostly chloroplasts) through a symmetric rolling-circle mechanism (Bruening et al., 1982; Hutchins et al., 1985; Daròs et al., 1994; Navarro et al., 1999). Reiterative transcription of the infecting (+) monomeric circular *(mc)* RNA by a nuclear-encoded polymerase (NEP) translocated into chloroplasts (Navarro et al., 2000) results in oligomeric head-to-tail (-) RNA intermediates, which after self-cleaving into monomeric linear *(ml)* forms via *cis*-acting hammerhead ribozymes (Hutchins et al., 1986) most likely acting co-transcriptionally (Carbonell et al., 2006), are circularized subsequently by a chloroplastic tRNA ligase (Nohales et al., 2012). The second half of the replication cycle, triggered by the *mc* (-) RNA, is the symmetric version of the first one (hence the name for this variant of the rolling-circle mechanism). Therefore, the two *mc* ASBVd (+) and (-) strands are physiologically relevant and the conformation they adopt *in vivo* are of particular interest because, lacking protein-coding ability, they should contain structural motifs crucial for different functions including replication and possibly trafficking.

The secondary structure of the *mc* ASBVd (+) and (-) RNAs has been analyzed *in silico* by searching those of minimal free energy (Symons, 1981; Hutchins et al., 1986; Gast et al., 1996; Navarro and Flores, 2000). While this thermodynamics-based methodology predicts rod-like or quasi-rod-like conformations for both strands, examination *in vitro* of the *ml* ASBVd (+) and (−) RNAs by selective 2′-hydroxyl acylation analyzed by primer extension (SHAPE), complemented by gel electrophoresis and other physical approaches (Delan-Forino et al., 2014; Giguère et

al., 2014; Hui-Bon-Hoa et al., 2014), has led to secondary structures exhibiting significant differences. Prominent among them is the presence (Delan-Forino et al., 2014) or absence (Giguère et al., 2014) of a kissing-loop interaction stabilizing the *ml* (−) RNA.

In the present work, besides re-assessing this discrepancy *in vitro* —but using the *mc* (+) and (-) forms instead of with their *ml* counterparts— we have applied *in vivo* SHAPE to address an intriguing conundrum: whether the predominant *mc* ASBVd (+) RNA exists *in planta* as a free nucleic acid or associated with host proteins that might provide some protection effect. Our results indicate that, resembling the situation reported recently for the *mc* (+) form of potato spindle tuber viroid (PSTVd), the type member of the family *Pospiviroidae* clustering the nuclear-replicating viroids (López-Carrasco and Flores, 2017), the *mc* ASBVd (+) form accumulates in its main subcellular habitat, the chloroplast (Mohamed and Thomas, 1980; Bonfiglioli et al., 1994; Lima et al., 1994; Navarro et al., 1999), essentially as a "naked" RNA. This finding has significant implications for the replication and survival strategy of ASBVd and other viroids in general.

RESULTS

The *mc* ASBVd (+) and (-) strands fold into rod- or quasi-rod-like conformations according to *in silico* predictions

Throughout the present study we have focused our attention on the *mc* ASBVd RNAs of both polarities because they are the forms that prime the two rolling-circles that operate in the symmetric replication of ASBVd. Moreover, in infected avocado, the *mc* ASBVd (+) form is by far the most abundant viroid RNA (Bruening et al., 1982; Hutchins et al., 1985; Daròs et al., 1994; Navarro and Flores, 2000), thus facilitating its analysis *in vivo* and its isolation and purification. The *mc* ASBVd (-) strand, although considerably less prevalent than its (+) counterpart, still reaches *in planta* a titer high enough to obtain the amount needed for dissection *in vitro* with several approaches. Previous thermodynamics-based predictions of the secondary structures of the *mc* ASBVd (+) and (-) RNAs, usually performed with the *Mfold*

software (Zuker, 2003), have led to rod-like conformations that in some cases include a short bifurcation in one of the terminal domains (Symons, 1981; Hutchins et al., 1986; Gast et al., 1996; Navarro and Flores, 2000). Here we have reassessed this issue with recent versions of the same software, and of two others, considering that the high A+U content of the *mc* ASBVd (+) and (-) forms should result in secondary structures of minimal free energy less stable and more difficult to predict than those typical of other viroids.

Concerning the *mc* ASBVd (+) RNA, the three softwares, *Mfold* (Zuker, 2003), *RNAfold* (Lorenz et al., 2011) and *RNAstructure* (Reuter and Mathews, 2010; Hajdin et al., 2013), the first two equipped with a version for circular RNAs, produced similar rod-shape secondary structures of minimal free energy for our variant, which differs in just one substitution (C213→U) from the reference variant (GenBank accession number J02020) (Symons, 1981). However, the conformations resulting from *Mfold* and *RNAstructure* presented in the left terminal domain a short bifurcation with two hairpins, one of them replaced by a large internal asymmetric loop in the conformation generated by *RNAfold* (Fig. 1a, inset 3). In addition, *Mfold* predicted two slightly different motifs (Fig. 1a, insets 1 and 2), the first one predicted also by *RNAfold* together with another one (Fig. 1a, insets 1 and 4). The probability profile created by *RNAstructure* differed along the rod-like structure, being higher in the terminal domains (particularly in the left one) than in the central domain (Fig. 1a).

With regard to the *mc* ASBVd (-) RNA, the three softwares produced the same rod-like conformation, thus providing strong support for it (Fig. 1b). As with the *mc* ASBVd (+) RNA, the probability pattern created by *RNAstructure* differed along the rod-like shaped conformation. A point worth of note is that the three softwares predicted a more stable conformation for the *mc* ASBVd (+) RNA ($\Delta G°$ between -73.8 and -69.3 kcal/mol) than for the *mc* ASBVd (-) RNA ($\Delta G°$ between -56.9 and -50.0 kcal/mol).

The *mc* ASBVd (+) and (-) forms adopt predominant secondary structures *in vitro* that can be discriminated by non-denaturing PAGE

We next tried to validate the *in silico* predictions and, particularly, whether the *mc* ASBVd (+) and (-) RNAs adopted a predominant conformation in solution and, in such a case, whether a physical distinction could be made between them. The *mc* ASBVd (+) form was directly isolated by denaturing PAGE from viroid-enriched RNA preparations from infected tissue; we assumed that the minor contamination with its co-migrating *mc* (-) counterpart, probably less than 10% (Daròs et al., 1994), should not interfere with the subsequent analysis. The *mc* ASBVd (-) form was prepared by circularization with a wheat germ extract of the *ml* ASBVd (-) RNA resulting from *in vitro* self-cleavage of a dimeric head-to-tail transcript.

Preliminary attempts to compare the structures in solution of the *mc* ASBVd (+) and (-) RNAs by non-denaturing PAGE in 5% gels failed to disclose a well-defined difference between their corresponding mobilities (data not shown). Although the *ml* (+) and (-) RNAs of eggplant latent viroid (ELVd, 333 nt) (Fadda et al., 2003) are clearly discriminated by electrophoresis in gels of this porosity (López-Carrasco et al., 2016), they might not have sufficient power to resolve RNAs of smaller size like those of ASBVd. Therefore, we performed our experiments in 8% gels in which, according to earlier data, *ml* ASBVd (+) and (-) RNAs migrate differentially (Delan-Forino et al., 2014). Considering that the *in vitro* SHAPE analysis to be carried out subsequently entails a thermal denaturation/renaturation, we also tested whether such treatment had any effect on the electrophoretic mobilities of *mc* ASBVd (+) and (-) RNAs with the same approach used before with two other viroids (López-Carrasco et al., 2016; López-Carrasco and Flores, 2017). In brief, prior to electrophoresis, two aliquots of each of the two RNAs under examination, re-suspended in water, were heated at 95 °C for 2 min and either snap-cooled on ice or slowly-cooled at 25 °C along 15 min, using a third non-treated aliquot as control. The samples were then brought to 37 °C for 5 min in the folding buffer (Wilkinson et al., 2006), with three other aliquots being similarly treated but with the folding buffer supplemented with 6 mM Mg^{2+}. In all instances the *mc* ASBVd (+) and (-) RNAs migrated as sharp bands, supporting their adoption of a predominant conformation *in vitro* (**Fig. 2A**), without dismissing the co-existence of others with minor changes undetectable by non-denaturing PAGE. The lack of noticeable Mg^{2+} effects did not

favor the presence of tertiary interactions like the kissing loops reported in PLMVd and CChMVd (Bussière et al., 2000; Gago et al., 2005).

Interestingly, compared with the size markers, the *mc* ASBVd (+) RNA migrated faster than its complementary *mc* (-) form, suggesting a more compact secondary structure for the former (Fig. 2b), a result that was confirmed by co-electrophoresis of mixed aliquots of the two RNAs (Fig. 2b). As indicated above, such observation is consistent with other made previously in gels of similar porosity, but using *ml* ASBVd (+) and (-) RNAs (Delan-Forino et al., 2014). However, when repeating this experiment, we found that while the *ml* ASBVd (-) RNA migrated in 8% gels as a sharp band, the *ml* ASBVd (+) RNA migrated as a blurred band (data not shown), thus hinting at the co-existence of different conformations in the latter. In contrast, the *mc* ASBVd (+) form adopted a predominant conformation as inferred from its defined electrophoretic mobility (Fig. 2). This observation shows that the circular structure provides enhanced stability, at least to the (+) strand, and reinforces the advantage of performing the analyses with the *mc* ASBVd (+) and (-) RNAs rather than with their *ml* counterparts, which may not display a similar behavior.

In vitro SHAPE with N-methylisatoic anhydride (NMIA) and 2-methylnicotinic acid imidazolide (NAI) corroborates the rod-like conformations predicted for the *mc* ASBVd (+) and (-) RNAs *in silico*

Migration of the *mc* ASBVd (+) and (-) RNAs as essentially single bands in non-denaturing PAGE was consistent with the existence in solution of predominant conformers for both polarity strands. To provide additional support for this idea at single-nucleotide resolution, we applied SHAPE *in vitro* with NMIA (Wilkinson et al., 2006) to the *mc* ASBVd RNAs purified from infected tissue by denaturing PAGE. We first used two individual primers in order to dissect the entire *mc* ASBVd (+) RNA, with the information gained serving to generate computer-assisted predictions with *RNAstructure* (Hajdin et al., 2013). Both primers produced mutually consistent data leading to a rod-shaped conformation very similar to that predicted *in silico* with *RNAfold* (Fig. 1a), thus containing in the left terminal domain a large internal asymmetric loop instead of the short bifurcation predicted by *RNAstructure* and

Mfold (Fig. 3a). Importantly, essentially the same conformation was obtained when NMIA was replaced by NAI, the alternative acylating reagent used for *in vivo* SHAPE (Kwok et al., 2013; Spitale et al., 2013; López-Carrasco and Flores, 2017) (Fig. 3b).

Subsequent application of *in vitro* SHAPE to the *mc* ASBVd (-) form, again with two separate primers to examine the whole RNA, resulted in basically the same rod-like secondary structure with NMIA and NAI (Fig. 4a and b), which additionally also coincided with that predicted by the three softwares *in silico* (Fig. 1b). On the other hand, the SHAPE reactivity of some nucleotides forming the lower strand of the left terminal loop (positions 123-128) did not support their involvement in a kissing-loop interaction with the lower strand of a right terminal loop (positions 231-236) (Fig. 4a and b), as proposed previously for a *ml* ASBVd (-) form (Delan-Forino et al., 2014).

The remarkable agreement between the *in silico* and *in vitro* approaches paved the way for addressing the next issue: whether the structure of the *mc* ASBVd (+) RNA *in planta* is also the same or different. For this aim we used NAI, which for SHAPE analyses *in vivo* is preferable to NMIA because of the higher $t_{1/2}$ hydrolysis of the former (Spitale et al., 2013).

SHAPE *in planta* shows that the *mc* ASBVd (+) form accumulates as a free RNA adopting a rod-shaped secondary structure without tightly bound host proteins

As indicated above we employed a NAI-based procedure (López-Carrasco and Flores, 2017), derived from a previous one (Spitale et al., 2013), substituting 5' primer labeling with radioactivity by a fluorophore. Moreover, as in our recent report with PSTVd (López-Carrasco and Flores, 2017), following NAI infiltration and incubation of ASBVd-infected leaves, and subsequent RNA extraction and clarification, the *mc* ASBVd RNAs were purified by denaturing PAGE. This step guaranteed that the observed SHAPE signals corresponded to stops taking place during reverse transcription of the *mc* ASBVd (+) RNA; the high amount of tissue (and NAI) needed made impractical to extend this analysis *in planta* to the *mc* ASBVd (-) RNA.

Because we assumed that a limiting factor could be the penetrability of the acylating reagent, we started our studies with expanding ASBVd-infected avocado leaves (8-10

cm in length), the cuticle of which was removed with ethylic ether before their infiltration with the NAI solution. However, the resulting signals produced by the *mc* ASBVd (+) RNA were very weak and difficult to reproduce. We next moved to flowers, which according to a previous report (Da Graça and Mason, 1983) and our own observations (data not shown), accumulate high levels of ASBVd. The SHAPE signals improved but were still unsatisfactory and, besides, this plant material was only available for a short period of time. Considering these results we returned to leaves, but of a very small size (2-3 cm in length), assuming that the NAI solution would penetrate more easily than in those of bigger size. That was indeed the case, with the SHAPE signals becoming clear and reproducible (Fig. 5). Finally, we carried out an additional control in which a preparation of *mc* PSTVd (+) RNA obtained from infected tissue was added immediately after homogenization of the ASBVd-infected tissue infiltrated with NAI. The ensuing SHAPE analysis of this external RNA control failed to reveal the reactivity observed previously *in vitro* (López-Carrasco and Flores, 2017) (data not shown), thus corroborating that acylation of the *mc* ASBVd (+) RNA occurred *in planta* and not *in vitro* during the subsequent manipulations.

Comparative analyses of the *in vitro* and *in vivo* data with NAI revealed that they were essentially identical, thus supporting that the *mc* ASBVd (+) RNA behaves in its physiological habitat as a free RNA folding into a rod-shaped conformation unprotected by firmly bound host proteins. In this conformation, wherein loops were generally more reactive than their flanking double-stranded helices, only two minor differences were detected: i) the upper strand of the asymmetric loop of the left terminal domain is formed by one single (A16) and by two nucleotides (A16 and G17) in the *in vitro* and *in vivo* structures, respectively, and ii) a small region delimited by C85 and A91 in the upper strand, and U152 and U160 in the lower strand, was slightly re-organized (Fig. 4 and 5).

DISCUSSION

For reasons explained elsewhere (Flores et al., 2012; López-Carrasco et al., 2016), viroid RNA conformations predicted *in silico* with algorithms minimizing the free-energy content, or determined *in vitro* with different biochemical and biophysical approaches, may not reproduce the conformation existing *in vivo.* The main of these reasons is that both *in silico* and in solution approaches neglect the effect that RNA-binding host proteins may have on the conformation of a viroid RNA in its physiological context. In addition, RNA secondary structure is constrained by transcription, steric crowding and interacting ions (Vandivier et al., 2016). Indeed, recent data indicate that the secondary structure of the *mc* (+) strand of a nuclear viroid (PSTVd) obtained by *in vivo* SHAPE, even if similar, is not identical to that observed by *in vitro* SHAPE, with the differences having been attributed to interactions with host proteins or to other factors present in the *in vivo* habitat (López-Carrasco et al., 2017).

Once resolved the global conformation *in vivo* of the *mc* (+) form of PSTVd, the type member of the family *Pospiviroidae* (López-Carrasco and Flores, 2017), application of the same methodology to a member of the family *Avsunviroidae* appeared the natural next step in order to test whether a general trend exist. Considering that SHAPE *in vivo* demands relatively high viroid titers in infected tissues, we discarded PLMVd (Hernández and Flores, 1992) and CChMVd (Navarro and Flores, 1997) due to their poor accumulation in *planta.* Between the remaining two members of the *Avsunviroidae,* ELVd (Fadda et al., 2003) and ASBVd (Symons, 1981), we chose the latter because despite being its natural host a woody plant, the isolate of this viroid with which we have been working along the years (GenBank accession number J02020 with the substitution C213→U) accumulates *in vivo* to levels comparable to the 5S ribosomal RNA (Bruening et al., 1982; Navarro and Flores, 2000), much higher than those reached by ELVd in eggplant.

Re-assessment of the most stable secondary structure predicted for the *mc* ASBVd (+) RNA by three softwares resulted in a similar rod-like conformation with minor deviations. This conformation, however, differed significantly in the distribution and size of some loops and double-stranded segments when compared with others reported previously (Symons, 1981; Hutchins et al., 1986; Gast et al., 1996; Navarro

and Flores, 2000). For the *mc* ASBVd (-) RNA the agreement was even better, with the three softwares predicting the same rod-shaped secondary structure. *In vitro* SHAPE of *mc* ASBVd (+) and (-) RNAs generated well-resolved structures that were almost identical with the two acylating reagents used (NMIA and NAI), in line with the adoption of predominant conformations by both RNAs *in vitro* as inferred from their migration as single bands in non-denaturing PAGE. These structures also agree with: i) those predicted *in silico,* particularly with the *RNAfold* software and, ii) those obtained previously by *in vitro* SHAPE (Giguère et al., 2014), while differing somewhat from others generated with the same approach (Delan-Forino et al., 2014). Furthermore, the rod-like conformations proposed *in vitro* for the *mc* ASBVd (+) and (-) RNAs are also consistent with the solubility in 2 M LiCl of the *mc* ASBVd RNAs extracted from infected tissue, mainly formed by the (+) strand (Navarro and Flores, 1997), and of the *ml* ELVd (+) and (-) RNAs resulting from *in vitro* self-cleavage that adopt quasi-rod-like secondary structures (López-Carrasco et al., 2016). Conversely, PLMVd and CChMVd RNAs, which fold into complex multi-branched conformations stabilized by a kissing-loop interaction, are insoluble under the same saline conditions (Navarro and Flores, 1997). In this same context, our *in vitro* SHAPE results do not support the existence in the *mc* ASBVd (-) RNA of the kissing-loop interaction proposed to stabilize a *ml* ASBVd (-) form (Delan-Forino et al., 2014), which has neither been inferred by *in vitro* SHAPE for another *ml* ASBVd (-) form (Giguère et al., 2014). Moreover, we have not detected by native PAGE any Mg^{2+}-induced difference in the mobility the *mc* ASBVd (-) RNA, while we have observed for it a slower mobility than for its (-) counterpart that also is Mg^{2+}-independent. This latter result, particularly, argues against the existence of a kissing-loop interaction in the *mc* ASBVd (-) RNA because an interaction of this kind in CChMVd causes a faster mobility consistent with a more compact folding (Gago et al., 2005), in contrasts with the results observed in the co-electrophoresis of the *mc* ASBVd (+) and (-) RNAs (Fig. 2b).

After some preliminary assays, we found that flowers, and particularly very small expanding leaves, were the most appropriate material for *in vivo* SHAPE, probably because they are easily penetrated by NAI. Moreover, this reagent has been

previously applied to determine the structure *in planta* of a chloroplast mRNA of *A. thaliana* (Kwok et al., 2013), thus indicating that NAI can traverse the membrane of this organelle. *In vivo* SHAPE of the *mc* ASBVd (+) form showed that it accumulates in chloroplasts as a free RNA uncovered by tightly bound host protein(s) which, like viral coat proteins, might exert a protecting role. However, as indicated before (López-Carrasco and Flores, 2017), the existence of loose or transient RNA-protein interactions, or of proteins interacting with double-stranded RNA motifs —in principle undetectable by SHAPE— cannot be dismissed, leaving apart that chemical approaches like SHAPE infer base pairing indirectly from the absence of reactivity (Vandivier et al., 2016). Pertinent to this context is the previous finding that UV irradiation of ASBVd-infected avocado leaves generates covalent adducts between the *mc* ASBVd (+) RNAs and host proteins, the most abundant of which, as revealed by tandem-mass spectrometry, are two chloroplast RNA-binding proteins (PARBP33 and PARBP35) of a family involved in stabilization, maturation and editing of chloroplasts transcripts. Moreover, PARBP33 behaves as an RNA chaperone that facilitates *in vitro,* and possibly *in vivo,* the self-cleavage of the oligomeric ASBVd intermediates resulting from rolling-circle replication (Daròs and Flores, 2002). UV light is a 'zero-length' cross-linking agent that promotes formation of covalent bonds between nucleic acids and proteins at their contact points, thus freezing the interaction existing *in situ* even if transient (Hockensmith et al., 1991; Pashev et al., 1991). Such cross-links, which demand close proximity and proper orientation between the reacting groups, may go unnoticed for *in vivo* SHAPE, highlighting the limitations of this latter approach and the need to combine physical and chemical strategies for proper dissection of host proteins interacting with viroid RNAs. In this regard, interactions of *mc* ASBVd RNAs with the host enzymes catalyzing replication may be also transient.

In summary, like the *mc* PSTVd (+) RNA (López-Carrasco and Flores, 2017), the *mc* ASBVd (+) RNA exists *in vivo* as free or "naked" RNA that folds into a rod-like conformation without strong association with host proteins. This finding attests to the common solution evolved by two different viroids that replicate and accumulate in two different subcellular compartments, the nucleus and chloroplast. The intrinsic

stability resulting from circularity and compact secondary structures promoted by double-stranded segments confer to these RNAs, and possibly to viroids in general, resistance to exonucleases and endonucleases, while some loops would play major functional roles as illustrated by the terminal A+U rich loops wherein the initiation sites of the ASBVd (+) and (-) strands have been mapped (Navarro and Flores, 2000). Relevant also to this framework is that there are more RNA sequences that fold into a closed than into an open structure of the same length, implying that the mutational robustness of closed structures is enhanced (Cuesta and Marubia, 2017).

MATERIALS AND METHODS

Extraction, clarification and examination of the *mc* ASBVd RNAs. These steps were performed as reported recently (López-Carrasco and Flores, 2017). In brief, total nucleic acid preparations from asymptomatic leaves from ASBVd-infected avocado plants *(Persea americana* Miller, cv. Fuerte) grown in a greenhouse, were obtained with water-saturated phenol and subsequently clarified using non-ionic cellulose and methoxyethanol. The *mc* ASBVd (+) and (-) RNAs were purified by double PAGE first in a non-denaturing 5% gel (acrylamide:bis-acrylamide ratio 39:1), with the segment demarcated by the DNA markers of 200 and 300 bp being excised and applied on top of a single-well 5% denaturing gel of the same porosity. The band of interest was cut and its RNAs gel-eluted overnight and examined by non-denaturing PAGE in 5% or 8% gels, the later with an acrylamide:bis-acrylamide ratio 19:1. The *mc* ASBVd (-) RNA was prepared by incubation at 25 °C for 2 h of gel-purified *ml* ASBVd (-) RNA (5 μg), resulting from *in vitro* self-cleavage of a dimeric head-to-tail transcript, in a final volume of 50 μl containing 25 μl of a wheat germ extract (Promega) and 40 U of the ribonuclease inhibitor from porcine liver (Takara).

Prediction of RNA structure *in silico*. Three softwares were applied to retrieve the structures of minimal free energy of the *mc* ASBVd (+) and (-) RNAs: *Mfold* version 4.7 (Zuker, 2003) and *RNAfold* included in the ViennaRNA package version 2.3.1 (Lorenz et al., 2011) using the circular versions and default parameters, and

RNAstructure version 5.8 (Shapeknots) (Reuter and Mathews, 2010; Hajdin et al., 2013) using the default parameters and beginning the numbering from the self-cleavage sites.

***In vitro* SHAPE**. The mixture of *mc* ASBVd (+) and (-) RNAs purified from infected avocado leaves were subjected to *in vitro* SHAPE with N-methylisatoic anhydride (NMIA, 13 mM in dimethyl-sulfoxide) essentially as described previously (Wilkinson et al., 2016; López-Carrasco and Flores, 2017), using 3 and 30 pmol of RNAs when analyzing the (+) and (-) forms, respectively. SHAPE *in vitro* with 2-methylnicotinic acid imidazolide (NAI, 50 mM in dimethyl-sulfoxide) was carried out similarly, being NAI prepared as reported before (Spitale et al., 2013). The resulting data were coupled to computer-assisted prediction (Hajdin et al., 2013). VIC-labeled fluorescent DNA primers (Applied Biosystems) RF-1370 (5'-CAGACCTGGTTTCGTC-3') and RF-1378 (5'-CCCTGAAAGGACGAAGTGATCAAGAG-3'), complementary to positions 57–42 and 174–149, respectively, and RF-1387 (5'-CTCTGAGTTTCGACTTGTGAGAGAAGG-3') and RF-1388 (5'-GATGGGAAGAACACTGATGAGTCTCGC-3') homologous to positions 72-98 and 178-204 respectively, were purified by denaturing PAGE in 20% gels. Extensions, sequencing reactions to identify the peaks, and resolution of the cDNAs by capillary electrophoresis were as detailed previously (Mortimer and Weeks, 2009; López-Carrasco and Flores, 2017). Electrophoregrams were examined with the QuShape software (Karabiber et al., 2013), which also normalized the reactivity data. At least three replicas were analyzed with each primer and acylating reagent, and the mean and standard deviation of the reactivity of each nucleotide was calculated.

***In vivo* SHAPE.** Young leaves (3 g) of different size (see Results) of ASBVd-infected avocado, pre-treated with ethylic ether to remove the cuticle, were mixed with 50 ml of buffer (40 mM HEPES-NaOH pH 7.5, 100 mM KCl, 0.5 mM $MgCl_2$) and gently shaken for 5 min. *In planta* acylation was triggered by incorporating NAI (100 mM in dimethylsulfoxide and just dimethylsulfoxide to the control reaction) and shaking the mixture at room temperature for 40 min. Following addition of β-

mercaptoethanol (500 mM) and shaking for another 10 min to stop the reaction, the leaves were drained and washed four times with water (100 ml). Extraction, purification, and primer-extension of the *mc* ASBVd (+) RNA was as with *in vitro* SHAPE. Six replicas were performed with each primer, and the mean and standard deviation of the reactivity of each nucleotide was estimated.

FUNDING INFORMATION

This work was supported by grant BFU2014-56812-P (to R.F.) from the Ministerio de Economía y Competitividad of Spain. A.L.C. was the recipient of a predoctoral fellowship from the same organism.

ACKNOWLEDGMENTS

We thank Drs. Cristina Romero and Alicia Barroso for their valuable help with the initial SHAPE experiments, Drs. Sonia Delgado and Pedro Serra for helpful advise, and A. Ahuir and M. Pedrote for excellent technical assistance.

CONFLICTS OF INTEREST

The authors declare that there is no conflict of interest.

REFERENCES

Bonfiglioli, R. G., McFadden, G. I. & Symons, R. H. (1994). In situ hybridization localizes avocado sunblotch viroid on chloroplast thylakoid membranes and coconut cadang-cadang viroid in the nucleus. *Plant J* **6,** 99-103.

Bruening, G., Gould, A. R., Murphy, P. J. & Symons, R. H. (1982). Oligomers of avocado sunblotch viroid are found in infected avocado leaves. *FEBS Lett* **148,** 71-78.

Bussière, F., Ouellet, J., Côté, F., Lévesque, D. & Perreault, J. P. (2000). Mapping in solution shows the peach latent mosaic viroid to possess a new pseudoknot in a complex, branched secondary structure. *J Virol* 74, 2647-2654.

Carbonell, A., De la Peña, M., Flores, R. & Gago, S. (2006). Effects of the trinucleotide preceding the self-cleavage site on eggplant latent viroid hammerheads: differences in co- and post-transcriptional self-cleavage may explain the lack of trinucleotide AUC in most natural hammerheads. *Nucleic Acids Res* **34,** 5613-5622.

Cuesta, J. A. & Manrubia, S. (2017). Enumerating secondary structures and structural moieties for circular RNAs. *J Theor Biol* (in press).

Da Graça, J. V. & Mason, T. E. (1983). Detection of avocado sunblotch viroid in flower buds by polyacrylamide-gel electrophoresis**.** *Phytopathol Z-J Phytopathol* **108,** 262-266.

Daròs, J. A., Marcos, J. F., Hernández, C. & Flores R. (1994). Replication of avocado sunblotch viroid: evidence for a symmetric pathway with two rolling circles and hammerhead ribozyme processing. *Proc Natl Acad Sci U S A* **91,** 12813-12817.

Daròs, J. A. & Flores, R. (2002). A chloroplast protein binds a viroid RNA *in vivo* and facilitates its hammerhead-mediated self-cleavage. *EMBO J* **21,** 749-759.

Delan-Forino, C., Deforges, J., Benard, L., Sargueil, B., Maurel, M. C. & Torchet C. (2014). Structural analyses of avocado sunblotch viroid reveal differences in the folding of plus and minus RNA strands. *Viruses* **6,** 489-506.

Diener, T. O. (2003). Discovering viroids—a personal perspective. *Nature Rev Microbiol* **1,** 75-80.

Fadda, Z., Daròs, J. A., Fagoaga, C., Flores, R. & Duran-Vila, N. (2003). Eggplant latent viroid (ELVd): candidate type species for a new genus within family *Avsunviroidae* (hammerhead viroids). *J Virol* **77,** 6528-6532.

Flores, R., Hernández, C., Martínez de Alba, E., Daròs, J. A. &, Di Serio, F. (2005). Viroids and viroid-host interactions. *Annu Rev Phytopathol* **43,** 117-139.

Flores, R., Serra, P., Minoia, S., Di Serio, F. & Navarro, B. (2012). Viroids: from genotype to phenotype just relying on RNA sequence and structural motifs. *Front Microbiol* **3,** 217.

Flores, R., Minoia, S., Carbonell, A., Gisel, A., Delgado, S., López-Carrasco, A., Navarro, B. & Di Serio, F. (2015). Viroids, the simplest RNA replicons: how they manipulate their hosts for being propagated and how their hosts react for containing the infection. *Virus Res* **209,** 136-145.

Gago, S., De la Peña, M. & Flores, R. (2005). A kissing-loop interaction in a hammerhead viroid RNA critical for its *in vitro* folding and *in vivo* viability. *RNA* **11,** 1073-1083.

Gast, F. U., Kempe, D., Spieker, R. L. & Sänger, H. L. (1996). Secondary structure probing of potato spindle tuber viroid (PSTVd) and sequence comparison with other small pathogenic RNA replicons provides evidence for central non-canonical base-pairs, large A-rich loops, and a terminal branch. *J Mol Biol* **262,** 652-670.

Giguère, T. Adkar-Purushothama, C. R., Bolduc, F. & Perreault, J. P. (2014). Elucidation of the structures of all members of the Avsunviroidae family. *Mol Plant Pathol* **15,** 767-779.

Hajdin, C. E., Bellaousov, S., Huggins, W., Leonard, C. W., Mathews, D. H. & Weeks, K. M. (2013). Accurate SHAPE-directed RNA secondary structure modeling, including pseudoknots. *Proc Natl Acad Sci U S A* **110,** 5498-5503.

Hernández, C. & Flores R. (1992). Plus and minus RNAs of peach latent mosaic viroid self-cleave *in vitro* via hammerhead structures. *Proc Natl Acad Sci U S A* **89,** 3711-3715.

Hockensmith, J. W., Kubasek, W. L., Vorachek, W. R., Evertsz, E. M. & von Hippel, P. H. (1991). Laser cross-linking of protein-nucleic acid complexes. *Methods Enzymol* **208,** 211-236.

Hui-Bon-Hoa, G., Kaddour, H., Vergne, J., Kruglik, S. G. & Maurel, M. C. (2014). Raman characterization of Avocado Sunblotch viroid and its response to external perturbations and self-cleavage. *BMC Biophys* **7,** 2.

Hutchins, C. J., Keese, P., Visvader, J. E., Rathjen, P. D., McInnes, J. L. & Symons, R. H. (1985). Comparison of multimeric plus and minus forms of viroids and virusoids. *Plant Mol Biol* **4,** 293-304.

Hutchins, C., Rathjen, P. D., Forster, A. C. & Symons, R. H. (1986). Self-cleavage of plus and minus RNA transcripts of avocado sunblotch viroid. *Nucleic Acids Res* **14,** 3627-3640.

Karabiber, F., McGinnis, J. L., Favorov, O. V. & Weeks, K. M. (2013). QuShape: rapid, accurate, and best-practices quantification of nucleic acid probing information, resolved by capillary electrophoresis. *RNA* **19,** 63-73.

Katsarou, K., Rao, A. L., Tsagris, M. & Kalantidis, K. (2015). Infectious long non-coding RNAs. *Biochimie* **117,** 37-47.

Kovalskaya, N. & Hammond, R. W. (2014). Molecular biology of viroid-host interactions and disease control strategies. *Plant Sci* **228,** 48-60.

Kwok, C. K., Ding, Y., Tang, Y., Assmann, S. M. & Bevilacqua, P. C. (2013). Determination of *in vivo* RNA structure in low-abundance transcripts. *Nat Commun* **4,** 2971.

López-Carrasco, A., Gago-Zachert, S., Mileti, G., Minoia, S., Flores, R. & Delgado, S. (2016). The transcription initiation sites of eggplant latent viroid strands map within distinct motifs in their *in vivo* RNA conformations. *RNA Biol* **13,** 83-97.

López-Carrasco, A. & Flores, R. (2017). Dissecting the secondary structure of the circular RNA of a nuclear viroid *in vivo:* a "naked" rod-like conformation similar but not identical to that observed *in vitro. RNA Biol* (in press, doi: 10.1080/15476286.2016.1223005).

Lorenz, R., Bernhart, S.H., Hoener zu Siederdissen, C., Tafer, H., Flamm, C., Stadler, P. F. & Hofacker, I. L. (2011). ViennaRNA Package 2.0. *Algorith Mol Biol* **6,** 26.

Lima, M. I., Fonseca, M. E. N, Flores, R. & Kitajima, E. W. (1994). Detection of avocado sunblotch viroid in chloroplasts of avocado leaves by in situ hybridization. *Arch Virol* **138,** 385-390.

Mohamed, N. A. & Thomas, W. (1980). Viroidlike properties of an RNA species associated with the sunblotch disease of avocados. *J Gen Virol* **46,** 157-167.

Mortimer, S. A. & Weeks, K. M. (2009). Time-resolved RNA SHAPE chemistry: quantitative RNA structure analysis in one second snapshots and at single nucleotide resolution. *Nature Protoc* **4,** 1413-1421.

Navarro, B. & Flores, R. (1997). Chrysanthemum chlorotic mottle viroid: unusual structural properties of a subgroup of viroids with hammerhead ribozymes. *Proc Natl Acad Sci U S A* **94,** 11262-11267.

Navarro, J. A., Darós, J. A. & Flores, R. (1999). Complexes containing both polarity strands of avocado sunblotch viroid: identification in chloroplasts and characterization. *Virology* **253,** 77-85.

Navarro, J. A. & Flores, R. (2000). Characterization of the initiation sites of both polarity strands of a viroid RNA reveals a motif conserved in sequence and structure. *EMBO J.* **19,** 2662-2670.

Navarro, J. A., Vera, A. & Flores, R. (2000). A chloroplastic RNA polymerase resistant to tagetitoxin is involved in replication of avocado sunblotch viroid. *Virology* **268,** 218-225.

Nohales, M. A., Molina-Serrano, D., Flores, R. & Daròs, J. A. (2012). Involvement of the chloroplastic isoform of tRNA ligase in the replication of viroids belonging to the family *Avsunviroidae. J Virol* **86,** 8269-8276.

Owens, R. A., Flores, R., Di Serio, F., Li, S. F., Pallás, V., Randles, J. W., Sano, T., Vidalakis, G. (2012). Viroids. In King, A. M. Q., Adams, M. J., Carstens, E. B. & Lefkowitz, E. J. (eds), *Virus Taxon: Ninth Rep Internatl Comm Taxon Viruses,* Elsevier/Academic Press, London UK, pp 1221-1234.

Palukaitis, P., Hatta, T., Alexander, D. M. & Symons, R. H. (1979). Characterization of a viroid associated with avocado sunblotch disease. *Virology* **99,** 145-151.

Palukaitis, P. (2014). What has been happening with viroids? *Virus Genes* **49,** 175-184.

Pashev, I. G., Dimitrov, S. I. & Angelov, D. (1991). Crosslinking proteins to nucleic acids by ultraviolet laser irradiation. *TIBS* **16,** 323-326.

Reuter, J. S. & Mathews, D. H. (2010). RNAstructure: software for RNA secondary structure prediction and analysis. *BMC Bioinform* **11,** 129.

Spitale, R. C., Crisalli, P., Flynn, R. A., Torre, E. A., Kool, E. T. & Chang, H. Y. (2013). RNA SHAPE analysis in living cells. *Nat Chem Biol* **9,** 18-20.

Steger, G. & Perreault, J. P. (2016). Structure and associated biological functions of viroids. *Adv Virus Res* **94,** 141-172.

Symons, R. H. (1981). Avocado sunblotch viroid: primary sequence and proposed secondary structure. *Nucleic Acids Res* **9,** 6527-6537.

Vandivier, L. E., Anderson, S. J., Foley, S. W. & Gregory, B. D. (2016). The conservation and function of RNA secondary structure in plants. *Annu Rev Plant Biol* **67,** 463-488.

Wilkinson, K. A., Merino, E. J. & Weeks, K. M. (2006). Selective 2'-hydroxyl acylation analyzed by primer extension (SHAPE): quantitative RNA structure analysis at single nucleotide resolution. *Nature Protoc* **1,** 1610-1616.

Zuker, M. (2003). Mfold web server for nucleic acid folding and hybridization prediction. *Nucleic Acids Res* **31,** 3406-3415.

Legends to figures

Fig. 1. Conformations of minimum free energy predicted for both strands of ASBVd (reference variant GenBank accession number J02020 with the substitution C213→U). (a) Quasi-rod-like secondary structure for the *mc* ASBVd (+) RNA predicted by *RNAstructure*. Insets (1) and (2), alternative motifs predicted by *Mfold,* and insets (1), (3) and (4) alternative motifs predicted by *RNAfold.* (b) Common rod-like secondary structure for the *mc* ASBVd (-) RNA predicted by *RNAstructure*, *RNAfold* and *Mfold.* In both panels the sequences forming the core of the hammerhead structures are delimited by flags, motifs conserved in natural hammerhead structures are within boxes, and self-cleavage sites are marked by arrows. The same numbers are used for both polarities. Colors in inset (5) denote the probability of nucleotides being double- or single-stranded as predicted by *RNAstructure.* The conformations serving as reference are those generated by *RNAstructure* because this is the software implemented in SHAPE.

Fig. 2. The *mc* ASBVd (+) and (-) RNAs show different mobilities in non-denaturing PAGE. (a) Before electrophoresis, aliquots of ASBVd (+) and (-) forms (upper and lower panels, respectively) were heated at 95 °C for 2 min and snap-cooled on ice (lane 2), gradually-cooled at 25 °C along 15 min (lane 3), or applied directly with no thermal treatment (NT) (lane 4). Three other aliquots of the same RNAs were processed similarly, but in the presence of 6 mM $MgCl_2$ (lanes 5, 6 and 7, respectively). (b) Aliquots of untreated ASBVd (+) and (-) RNAs were loaded separately (lanes 2 and 4, respectively) or mixed together (lane 3). Three other aliquots of the same RNAs were processed similarly, but in the presence of 6 mM $MgCl_2$ (lanes 5, 6 and 7, respectively). M refers to DNA markers with their size (in base pairs) indicated on the left (lanes 1). Gels were stained with ethidium bromide and are shown in the inverted option to facilitate visualization.

Fig. 3. *In vitro* SHAPE with NMIA (a) and NAI (b) leads to essentially the same rod-like secondary structure for the *mc* ASBVd (+) RNA. This conformation is very

similar to that predicted *in silico* with *RNAfold* and contains a large internal asymmetric loop in the left terminal domain. Nucleotides in red, yellow and black displayed high (more that 0.85), intermediate (0.85-0.40) and low (less than 0.40) SHAPE-reactivity. Other details as in the legend to Fig. 1.

Fig. 4. *In vitro* SHAPE with NMIA (a) and NAI (b) also predicts the same rod-like secondary structure for the *mc* ASBVd (-) RNA. This conformation additionally coincides with that predicted by the three softwares *in silico.* Other details as in the legends to Fig. 1 and 3.

Fig. 5. *In vivo* SHAPE confirms a rod-like conformation for the *mc* ASBVd (+) RNA. (a) Results obtained with NAI *in vivo* coupled to computer-assisted prediction using *RNAstructure*. (b) Results obtained with the same acylating agent *in vitro* (see Fig. 3b) are included here to facilitate a direct comparison. Other details as in the legends to Fig. 1 and 3.

(a)

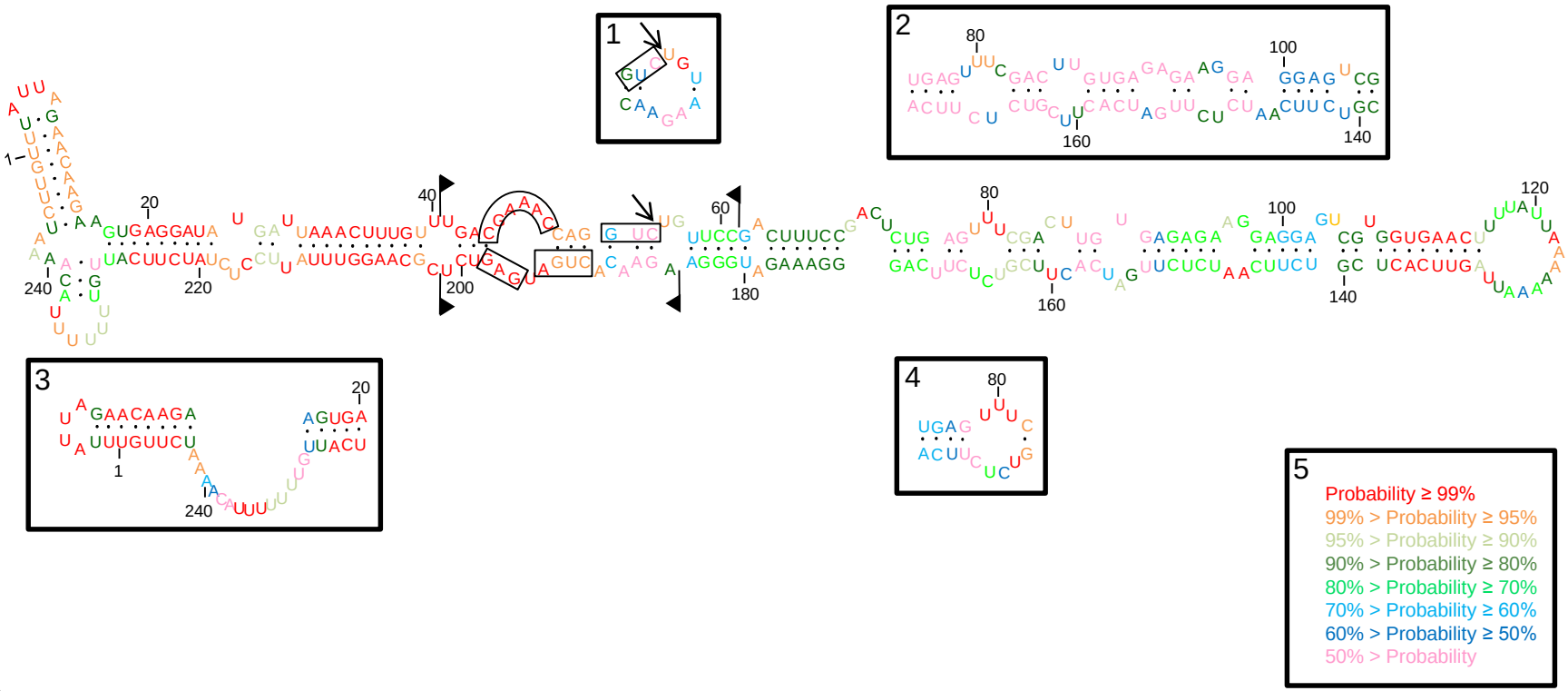

(b)

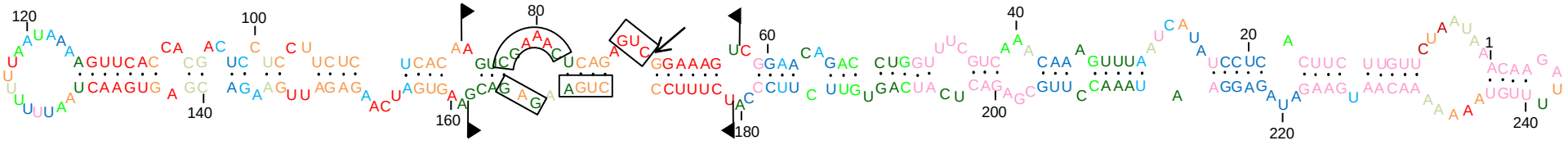

Figure 1

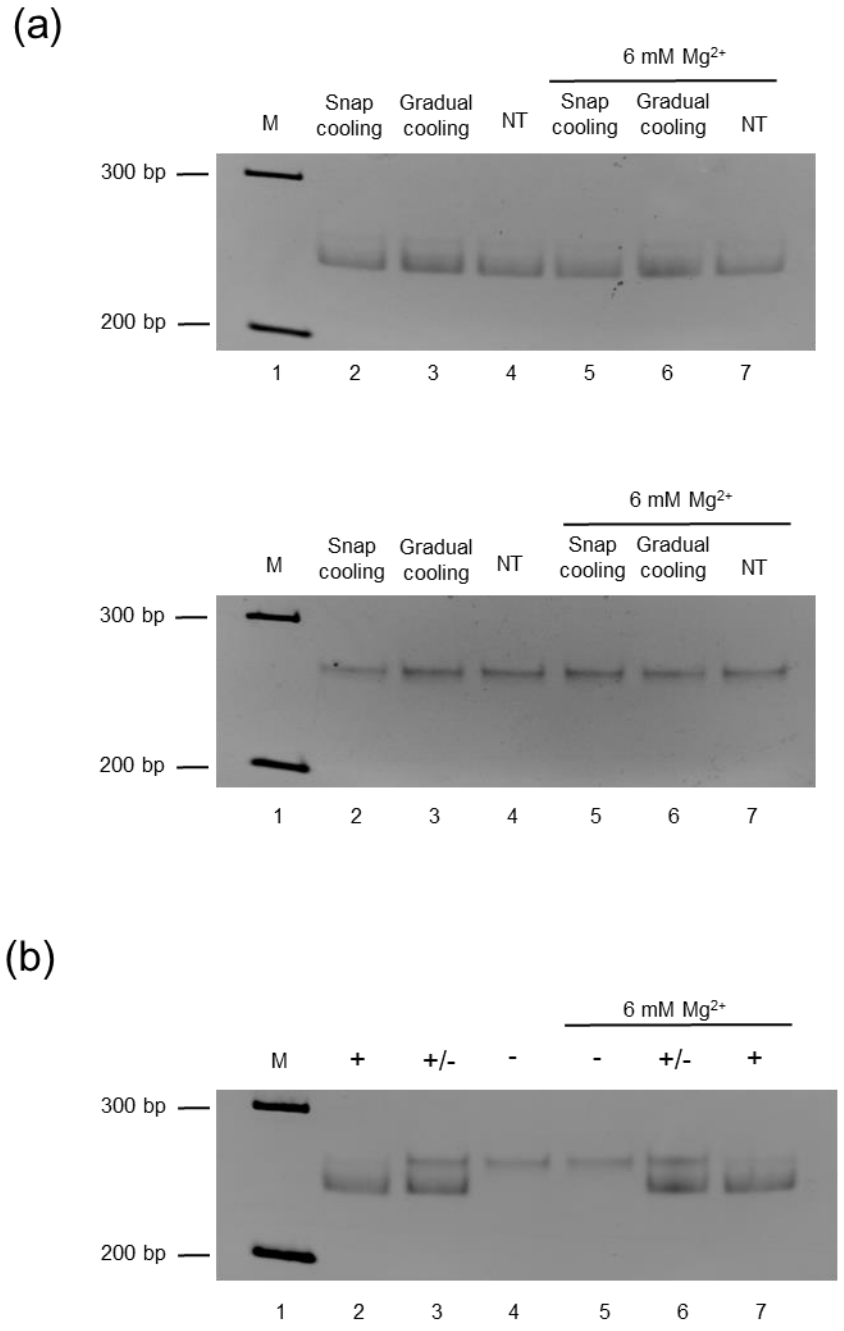

Figure 2

(a)

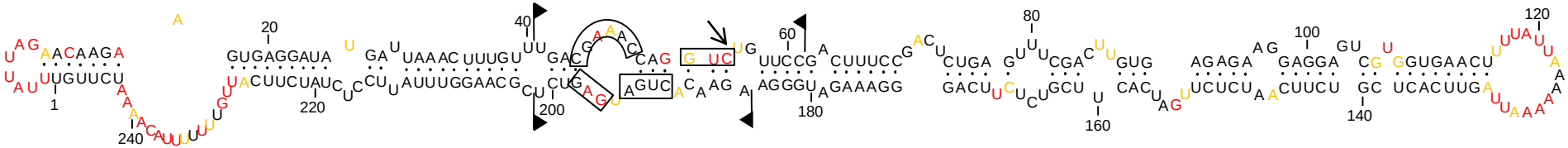

(b)

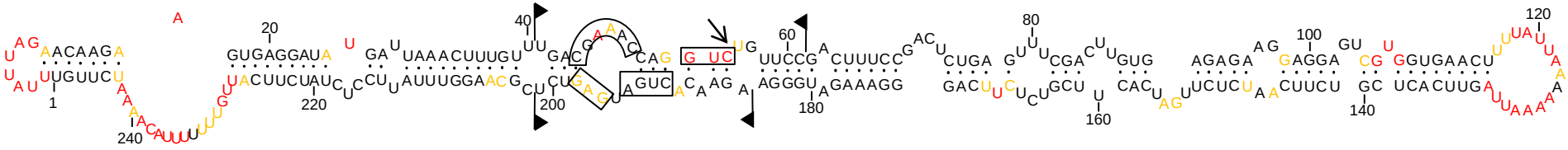

Figure 3

(a)

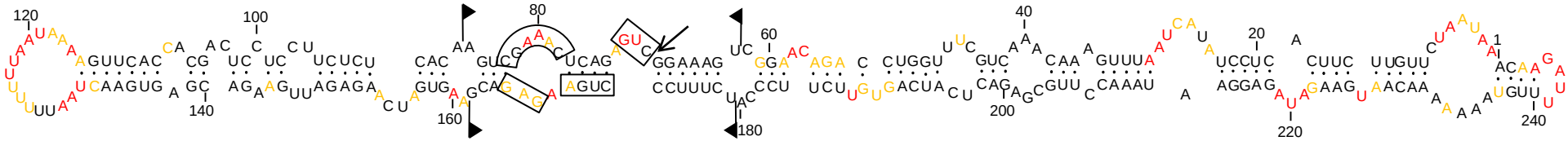

(b)

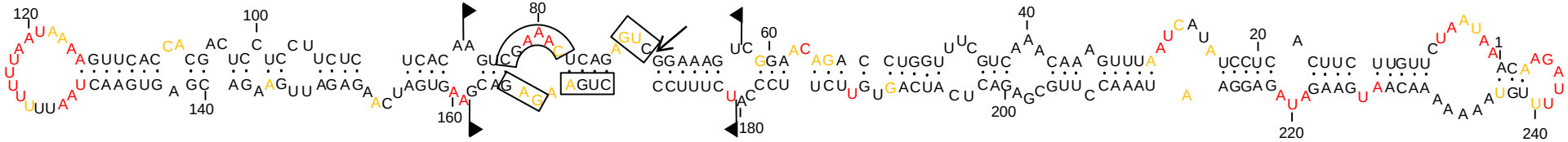

Figure 4

(a)

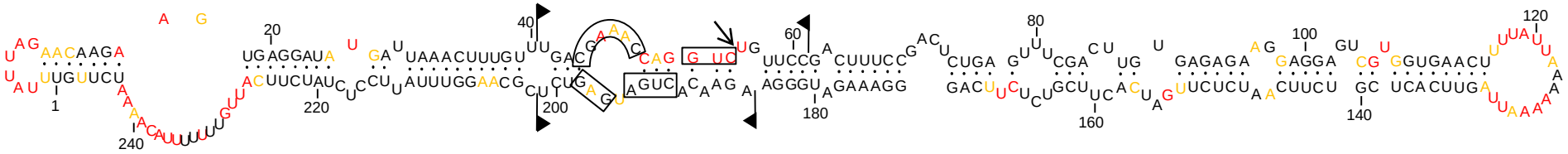

(b)

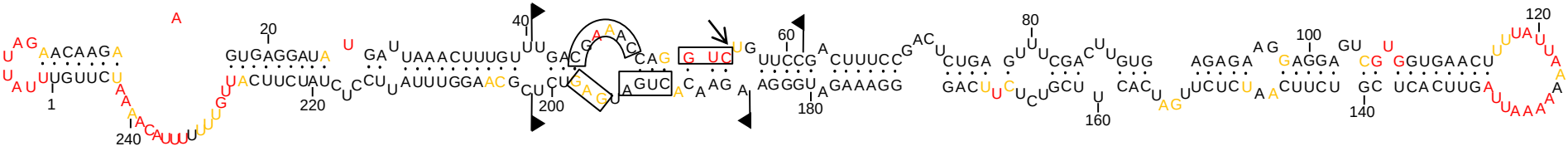

Figure 5